

Anisotropic magnetoresistance of GaAs two-dimensional holes

S. J. Papadakis, E. P. De Poortere, and M. Shayegan

Department of Electrical Engineering, Princeton University, Princeton, New Jersey 08544, USA.

R. Winkler

Institut für Technische Physik III, Universität Erlangen-Nürnberg, Staudtstr. 7, D-91058 Erlangen, Germany.

(February 1, 2020)

Experiments on high-quality GaAs (311)A two-dimensional holes at low temperatures with in-plane magnetic fields (B) reveal positive magnetoresistance whose details depend on the direction of B relative to both the crystal axes and the current direction. The value of B at which the resistivity is nearly temperature-independent also depends on the orientation of B . To explain the data, the coupling of the orbital motion to B , as well as the anisotropic band structure of the holes and a re-population of the spin-subbands in the presence of B , need to be taken into account.

71.30.+h, 71.70.Ej, 73.50.-h

There has been interest recently in the ground state of a disordered two-dimensional (2D) carrier system. Twenty years ago, scaling arguments and supporting experimental data indicated that at temperature $T = 0$ K such a system must be insulating [1,2]. However, prompted by new data in Si 2D electrons [3] and subsequently multiple different 2D carrier systems [4], revealing a metallic-like behavior, this question is being revisited both experimentally and theoretically [5–7].

One specific area of interest has been the spin degree of freedom [8–10] and the effect of an in-plane magnetic field (B) on the metallic behavior [11–14]. Recent calculations have pointed out the importance of spin-orbit coupling [6] and, in 2D systems with finite layer thickness, the coupling of the orbital motion to B [7]. Both have predicted an anisotropy in the magnetoresistance (MR) depending on the orientation of sample current I with respect to B . Motivated by these predictions, we have measured the MR of a high-mobility 2D hole system (2DHS) in a GaAs (311)A quantum well. The 2DHS density range was such that at $B = 0$ the sample resistivity (ρ) showed metallic T -dependence. MR measurements were made with an in-plane B parallel to the $[\bar{2}33]$ and $[01\bar{1}]$ crystal axes, and with I parallel to and perpendicular to the applied B for each case. In all cases the data show positive MR, consistent with the predictions of Ref. [7]. However, we observe a striking dependence of the MR on the orientation of B relative to the crystal axes. We show that this dependence is linked to the anisotropy of the 2DHS band structure and a re-population of the spin-subbands with increasing B .

The samples are Si-modulation doped GaAs quantum wells grown on (311)A GaAs substrates. Even at $B = 0$, these samples exhibit a mobility anisotropy believed to be due to an anisotropic surface morphology (see [15,16] and references therein). The interfaces between the GaAs quantum well and the AlGaAs barriers are believed to be corrugated, with ridges along the $[\bar{2}33]$ direction which reduce the mobility for $I \parallel [01\bar{1}]$. While the metallic behavior has been studied in this system extensively, little

attention has been paid so far to the differences between transport along $[01\bar{1}]$ and $[\bar{2}33]$.

Our sample is patterned with an L-shaped Hall bar aligned along $[01\bar{1}]$ and $[\bar{2}33]$ to allow simultaneous measurement of the resistivities along the two directions. The sample has metal front and back gates to control both the 2DHS density (p) and the perpendicular electric field (E_{\perp}) applied to the well [9,10]. Measurements are done in dilution and pumped ^3He refrigerators with B up to 16 T. In the ^3He refrigerator, the sample is mounted on a single-axis tilting stage that can be rotated *in-situ* to change the plane of the 2DHS from perpendicular to parallel to the applied B . Figure 1(a) demonstrates the high quality of the 2DHS in this sample.

The $[01\bar{1}]$ and $[\bar{2}33]$ directions of (311)A GaAs typically have mobilities μ that differ by as much as a factor of three [15,9]. For the present sample, at 30 mK and $p = 6.3 \times 10^{10} \text{ cm}^{-2}$, we have $\mu_{[01\bar{1}]} = 425,000 \text{ cm}^2/\text{Vs}$ and $\mu_{[\bar{2}33]} = 530,000 \text{ cm}^2/\text{Vs}$. As illustrated in Fig. 1(b), the T -dependence of ρ is also significantly different along the two directions in the density range where the behavior is metallic. The $[01\bar{1}]$ direction typically shows a larger fractional change in ρ , $\rho(T)/\rho(30 \text{ mK})$, than the $[\bar{2}33]$ direction, as T is increased [9,10]. This suggests that the scattering mechanisms associated with the two mobility directions have different T dependencies, and that the orientation of I relative to the crystal axes is an important parameter in understanding the data.

Figure 2 shows ρ at $T = 0.3$ K as a function of B applied in the plane of the 2DHS. The left (right) column shows data for $I \parallel [01\bar{1}]$ ($I \parallel [\bar{2}33]$), with the in-plane B both parallel and perpendicular to I . To obtain these data, on separate cooldowns the sample was mounted with the $[01\bar{1}]$ or the $[\bar{2}33]$ crystal axis parallel to the tilt axis. The density p was deduced from the Hall coefficient by measuring the transverse MR in a B perpendicular to the plane of the 2DHS. The stage was then tilted to make the 2DHS plane parallel to the applied B , and the MR was measured. The front and back gates were used to change p . For $I \parallel [01\bar{1}]$, ρ is always larger when $I \perp B$.

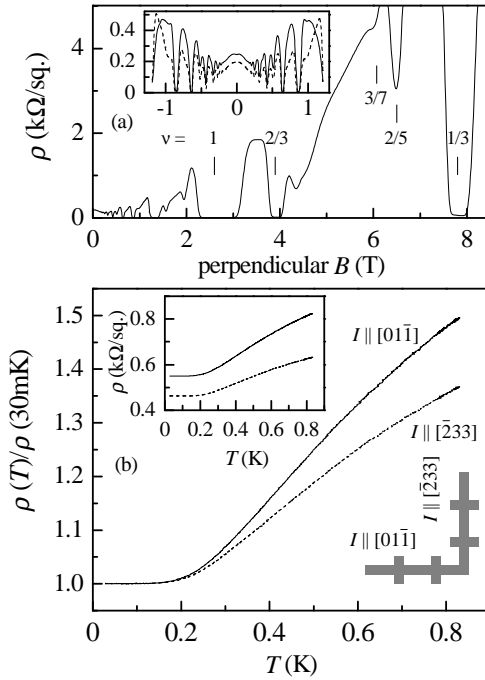


FIG. 1. (a) Resistivity ρ data for magnetic field B perpendicular to the plane of the 2D hole system with a density $p = 6.3 \times 10^{10} \text{ cm}^{-2}$ and current $I \parallel [\bar{2}33]$ at $T = 30 \text{ mK}$. The data exhibits fractional quantum Hall effect at low filling factors (ν), demonstrating the high quality of the sample. The inset shows low- B data for $I \parallel [01\bar{1}]$ (solid trace) and $I \parallel [\bar{2}33]$ (dashed trace). (b) $B = 0$ temperature-dependence at $p = 3.3 \times 10^{10} \text{ cm}^{-2}$, highlighting the difference between $[01\bar{1}]$ (solid) and $[\bar{2}33]$ (dashed) directions. The main figure shows the fractional change in ρ as T is increased, while the inset shows the raw data. The schematic at lower right depicts the Hall bar used for the measurements.

However, the $I \parallel [\bar{2}33]$ data are qualitatively different: at low B and p , the $I \perp B$ traces have lower ρ , and cross the $I \parallel B$ traces at higher B .

In Fig. 2, there are pronounced qualitative similarities between the dashed traces on the right and the solid traces on the left, and vice versa. To highlight these similarities, in Fig. 3 we show the fractional change in ρ , $\rho(B)/\rho(B = 0)$, for B along the $[\bar{2}33]$ (left column) and $[01\bar{1}]$ (right column) directions. Plotting this way, a striking similarity is evident in the qualitative features of the traces with the same B orientation relative to the crystal axes, even though the I orientations are different. All traces start with a small slope and curve upwards. Then there is an inflection point followed by a reduction in slope, followed by another inflection point beyond which the traces curve upwards again. To highlight this behavior, the arrows in Fig. 3 are placed between the two inflection points, at a B we will refer to as B^* . Surprisingly, for each p , B^* for the $B \parallel [\bar{2}33]$ traces is about 4 T smaller than for the $B \parallel [01\bar{1}]$ traces, regardless of the I

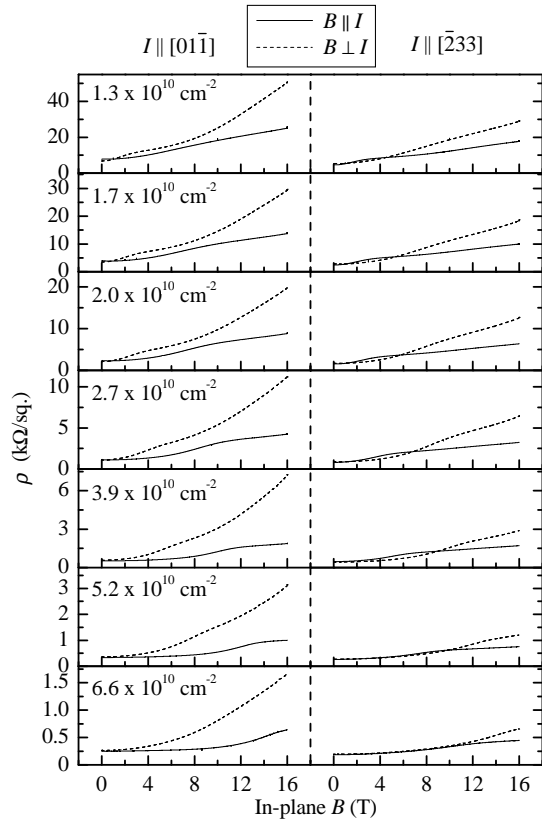


FIG. 2. Magnetoresistance at $T = 0.3 \text{ K}$ in an in-plane B , showing how resistivity changes as the orientation of B is changed from parallel to perpendicular to the current (I) direction. The density p is listed in each panel.

direction. Also, B^* becomes smaller as p is reduced. Figure 3 reveals that the relative orientations of B and the crystal axes play an important role in the MR features.

Figure 4 shows the T -dependence of MR at $p = 3.9 \times 10^{10} \text{ cm}^{-2}$, for the four measured relative orientations of B , I , and crystal axes. For each panel, the traces exhibit a nearly T -independent magnetic field B_T which occurs near the trace's first inflection point. This is consistent with the data of Ref. [14]. For $B < B_T$, the data show metallic behavior, and for $B > B_T$, insulating behavior. B_T is different in each panel, and it changes much more for a rotation of the crystal axes relative to B than it does for a rotation of I relative to B .

The existence of the MR features around B^* is intriguing. Similar, though sharper, features have been observed in in-plane B measurements in systems with multiple confinement subbands when a subband is depopulated [17]. Similarly, the features in our data may be related to the changes in the relative populations of the spin-subbands and the resulting changes in subband mobility and inter-subband scattering as the in-plane B is increased. The T -dependence data are consistent with this hypothesis as they show that B_T , like B^* , depends much more strongly on the orientation of the crystal axes relative to B than on the orientation of I relative to B .

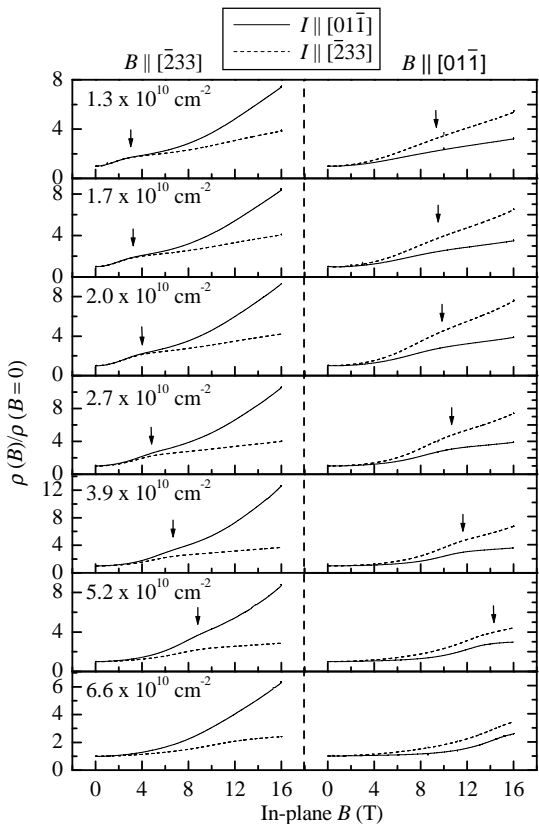


FIG. 3. Fractional change in resistivity due to an in-plane B , showing that the relative orientations of B and the crystal axes play an important role in determining the position of the magnetoresistance features. The vertical arrows mark B^* as defined in the text.

Spin-subband populations should not be related to the I direction in a 2D system, but as we will demonstrate below, can depend on the orientation of B relative to the crystal axes.

To test if the MR features around B^* are related to the spin-subband de-population, we have done self-consistent subband calculations with no adjustable parameters [18] that give us spin-subband densities as a function of in-plane B (Fig. 5). Figure 5 shows that the upper spin-subband de-populates more quickly for $B \parallel [\bar{2}33]$ than for $B \parallel [01\bar{1}]$ [19]. This is consistent with the experimental observation that B^* is smaller for $B \parallel [\bar{2}33]$. Also, the B at which the subband completely de-populates changes with p in much the same way as B^* does. However, B^* is significantly smaller than the field at which the calculations show the upper spin-subband to reach zero density. We believe that the real spin-subband de-population occurs at a lower B than the band calculations predict because hole-hole interaction enhances the effective mass m^* and effective g -factor g^* in a dilute 2D system like ours. The average hole spacing in units of effective Bohr radius, r_s , for our experiment ranges from $r_s = 6.9$ to 15.6 for $p = 6.6 \times 10^{10} \text{ cm}^{-2}$ to $1.3 \times 10^{10} \text{ cm}^{-2}$ [20]. Okamoto *et al.* [13], conclude that for Si 2D electrons

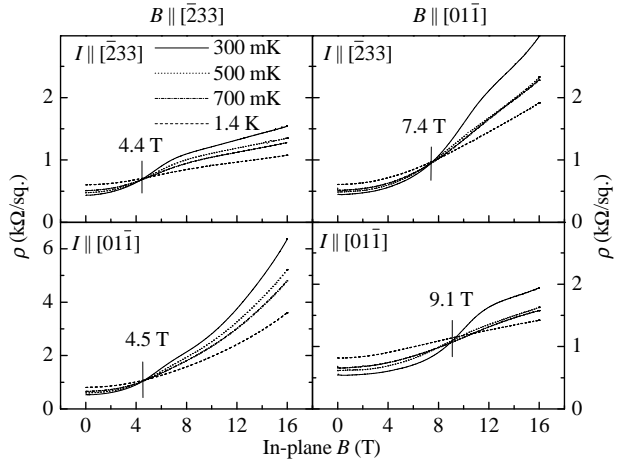


FIG. 4. Magnetoresistance data at various temperatures, for density $p = 3.9 \times 10^{10} \text{ cm}^{-2}$, for the four relative orientations of B , I , and crystal axes. The fields B_T at which the resistivity is nearly T -independent are indicated by vertical marks.

with r_s in this range, g^*m^* is enhanced by a factor of 2.7 to 5.5. Assuming similar enhancement in our samples, we would expect a reduction by the same factor of B required to de-populate a subband. Using these numbers to adjust the de-population field given by the band calculations would put it near B^* , strongly suggesting that the MR features are due to spin-subband de-population. Combining this observation with the T -dependence data, we conclude in agreement with the results of Ref. [13] that the existence of two populated spin-subbands is required for metallic behavior.

In the data of Ref. [13], and likely in ours, the spin-subband de-population occurs at the second inflection point in the MR data. However, B_T , above which there is insulating behavior, is smaller than this value. This may be because the low-density spin-subband stops playing a role in transport when its mobility μ becomes sufficiently low, before it is fully de-populated.

Further evidence linking the MR features to spin-subband de-population is provided by our data at constant p with changing E_\perp . The degree of asymmetry in the potential that confines the carriers to 2D controls the spin-splitting, and plays an important role in the magnitude of the $B = 0$ temperature-dependence of the resistivity [9,10]. For the data in Figs. 2 and 3, E_\perp is kept within 1 kV/cm of 5 kV/cm. This E_\perp is included in the calculations plotted in Fig. 5. Measurements at a constant $p = 3.9 \times 10^{10} \text{ cm}^{-2}$ as E_\perp is increased from 4.5 kV/cm to 12.5 kV/cm reveal that B^* and B_T shift to higher B by about 2 T. This observation is in agreement with the calculations done at fixed p for varying E_\perp . The T - and E_\perp -dependencies also demonstrate that for a fixed p and B , the behavior can be driven from metallic to insulating by changing E_\perp alone.

At higher in-plane B , beyond the MR features around B^* , the data are qualitatively similar. The traces for

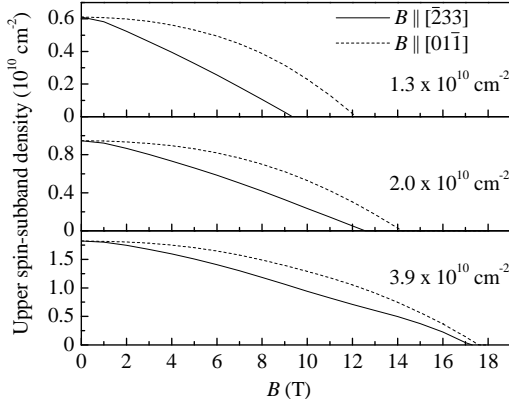


FIG. 5. Results of self-consistent calculations showing the upper spin-subband density with increasing in-plane B . Note the significant difference between curves for $B \parallel [233]$ and for $B \parallel [01\bar{1}]$.

$B \perp I$ have greater slope than the corresponding traces with $B \parallel I$, regardless of crystal axes. In this regime the magnetic confinement can become comparable to the electric confinement, and the effects due to the finite-thickness of the 2DHS may be dominant. Ref. [7] then predicts that MR with in-plane B should be significantly larger for $B \perp I$ than for $B \parallel I$, in agreement with our highest B data. The data in which E_{\perp} is changed at constant p support this interpretation as well. As E_{\perp} is increased, the confining potential becomes narrower, and the thickness of the 2DHS decreases. This should increase the B required for finite-thickness effects to become important, and the data show that the MR anisotropy at $B = 16$ T is smaller for larger E_{\perp} .

In summary, we have shown that a (311)A GaAs 2D hole system in the metallic regime exhibits a positive magnetoresistance due to in-plane B . This is qualitatively consistent with a model in which the holes' orbital motion due to the finite thickness of the 2D layer couples with the applied B [7]. Furthermore, the details of the magnetoresistance reveal surprisingly that the relative orientations of B , I , and the crystal axes are all important in the expression of in-plane magnetoresistance through their effects on the spin-subband densities. Our data, in agreement with the results of Ref. [13] for 2D electrons in Si, suggest that the metallic behavior in GaAs 2D holes is observed only when two spin-subbands are occupied. This conclusion is also consistent with our previous data [9,10] which revealed that the presence of two spin-subbands with different populations appears to be linked to the metallic behavior.

This work was supported by the NSF and ARO. We thank M. Hofmann for stimulating discussions.

- [1] E. Abrahams, P. W. Anderson, D. C. Licciardello, and T. V. Ramakrishnan, Phys. Rev. Lett. **42**, 673 (1979).
- [2] D. J. Bishop, D. C. Tsui, and R. C. Dynes, Phys. Rev. Lett. **44**, 5737 (1980).
- [3] S. V. Kravchenko, G. V. Kravchenko, and J. E. Furneaux, Phys. Rev. B **50**, 8039 (1994); S. V. Kravchenko, D. Simonian, M. P. Sarachik, W. Mason, and J. E. Furneaux, Phys. Rev. Lett. **77**, 4938 (1996).
- [4] D. Popović, A. B. Fowler, and S. Washburn, Phys. Rev. Lett. **79**, 1543 (1997); P. T. Coleridge, R. L. Williams, Y. Feng, and P. Zawadzki, Phys. Rev. B **56**, R12764 (1997); J. Lam, M. D'Iorio, D. Brown, and H. Lafontaine, Phys. Rev. B **56**, R12741 (1997); Y. Hanein *et al.*, Phys. Rev. Lett. **80**, 1288 (1998); M. Y. Simmons *et al.*, Phys. Rev. Lett. **80**, 1292 (1998); S. J. Papadakis and M. Shayegan, Phys. Rev. B **57**, R15068 (1998).
- [5] V. Dobrosavljević, E. Abrahams, E. Miranda, and S. Chakravarty, Phys. Rev. Lett. **79**, 455 (1997); V. M. Pudalov, Pis'ma Zh. Èksp. Teor. Fiz. **66**, 168 (1997) [JETP Lett. **66**, 175 (1997)]; B. L. Altshuler and D. Maslov, Phys. Rev. Lett. **82**, 145 (1999); S. Das Sarma and E. H. Hwang, Phys. Rev. Lett. **83**, 164 (1999).
- [6] G. H. Chen, M. E. Raikh, and Y. S. Wu, cond-mat/9904451.
- [7] S. Das Sarma and E. H. Hwang, cond-mat/9909452.
- [8] V. M. Pudalov, G. Brunthaler, A. Prinz, and G. Bauer, Pis'ma Zh. Èksp. Teor. Fiz. **65**, 168 (1997) [JETP Lett. **65**, 932 (1997)].
- [9] S. J. Papadakis *et al.*, Science **283**, 2056 (1999).
- [10] S. J. Papadakis *et al.*, to be published in Physica E.
- [11] D. Simonian, S. V. Kravchenko, M. P. Sarachik, and V. M. Pudalov, Phys. Rev. Lett. **79**, 2304 (1997).
- [12] K. M. Mertes *et al.*, Phys. Rev. B **60**, R5093 (1999).
- [13] T. Okamoto, K. Hosoya, S. Kawaji, and A. Yagi, Phys. Rev. Lett. **82**, 3875 (1999).
- [14] J. Yoon *et al.*, cond-mat/9907128.
- [15] J. J. Heremans, M. B. Santos, K. Hirakawa, and M. Shayegan, J. Appl. Phys. **76**, 1980 (1994).
- [16] M. Wassermeier *et al.*, Phys. Rev. B **51**, 14721 (1995).
- [17] J. Jo *et al.*, Phys. Rev. B **47**, 4056 (1993).
- [18] R. Winkler and U. Rössler, Phys. Rev. B **48**, 8918 (1993); G. Goldoni and A. Fasolino, Phys. Rev. B **48**, 4948 (1993).
- [19] For $B = 0$ the upper spin-subband density is smaller than half the p because of the inversion-asymmetry-induced spin splitting of the subband states [9].
- [20] To calculate r_s we use an unenhanced $m^* = 0.2m_e$ [B. E. Cole *et al.*, Phys. Rev. B **55**, 2503 (1997)]. In our calculations we obtain a density-of-states m^* at $B = 0$ with approximately the same value.